Study of Forbush Decreases with IceTop

THE ICECUBE COLLABORATION[1]
[1]*See special sections in these proceedings*

Abstract: IceTop, the surface component of the IceCube neutrino observatory, is an air shower array installed at the Amundson-Scott South Pole station. It consists of 162 ice Cherenkov detectors, each 90 cm deep with surface area 2.7 m^2. The tanks detect secondary particles produced by cosmic rays interacting in the atmosphere with a counting rate exceeding 1 kHz per detector. The statistical precision enabled by the high counting rate of the array enables the study of cosmic ray heliospheric disturbances with unprecedented time resolution in the multi-GeV energy regime. Since the detector has each different threshold settings, it is also possible to estimate the energy spectrum of particles in such events. We illustrate the performance during a Forbush decrease observed in February, 2011.

Corresponding authors: Takao Kuwabara[2] (*takao@bartol.udel.edu*), Paul Evenson[2] (*evenson@udel.edu*)
[2]*Bartol Research Institute and Dept. of Physics and Astronomy, University of Delaware, Newark, DE 19716, U.S.A.*

Keywords: IceCube, IceTop, Forbush decrease

1 Introduction

IceTop, the surface component of the IceCube neutrino observatory, is located at the Amundson-Scott station near the geographic South Pole (altitude 2835m). It is an air shower array consisting of 162 ice Cherenkov detectors, each 90 cm deep with surface area 2.7 m^2. Signals are recorded by photomultipliers in two Digital Optical Modules (DOMs) frozen into the ice in each detector. Two DOMs in a detector are typically operated at high and low gain settings to provide appropriate dynamic range. In this paper we consider only data from the set of 146 "high gain" DOMs that were deployed prior to the 2010-11 austral summer. The large detector volume coupled with the high altitude and nearly zero geomagnetic cutoff at the South Pole yield an extremely high counting rate that allows the study of cosmic ray time variations with unprecedented accuracy.

This analysis uses counting rates from the two discriminators in the high gain DOMs. They are termed SPE (Single Photo Electron), and MPE (Multi Photo Electron) for historical reasons. The SPE discriminators are actually set to thresholds ranging between 1 and 20 photoelectrons whereas the MPE threshold are all set near 20 photoelectrons. The counting rates at those SPE and MPE threshold settings range from 1 to 10 kHz. IceTop detectors respond to several components of the secondaries (muons, neutrons, and electomagnetic components [1]) produced by interactions of >0.6 GeV primary cosmic rays with Earth's atmosphere, and the signal spectrum of the detector contains information on the spectrum of the primary particles. By observing the intensity variation at different threshold settings we can estimate the energy spectrum of primary particles during the heliospheric events.

At energies up to $\sim$100 GeV, primary galactic cosmic rays experience significant variations in response to passing solar wind disturbances such as interplanetary coronal mass ejections (ICMEs). ICMEs consist of large eruptions of magnetic field and plasma from Sun. ICMEs accompanied by a strong shock often have a depleted region of galactic cosmic rays behind the shock and within the CME. When Earth enters this depleted region, ground-based cosmic ray detectors record a "Forbush Decrease" [2]. During the decrease the cosmic ray intensity fluctuates in response to magnetic structures embedded in the ICME. Data with high statistical precision from IceTop allow study of these structures with unprecedented time resolution, coupled with simultaneous spectral information. In this paper, we illustrate the performance of IceTop during a Forbush decrease event observed on 18 February 2011.

2 Observation of 18 February 2011 Forbush Decrease

The 18 February 2011 Forbush decrease, related to the X2.2 solar flare that occurred on 15 February 01:44 UT, was the largest Forbush decrease since December 2006. A summary of observations of this decrease is shown in Figure 1. The four top panels display solar wind speed, total component (Bt) and North-South component (Bz) of

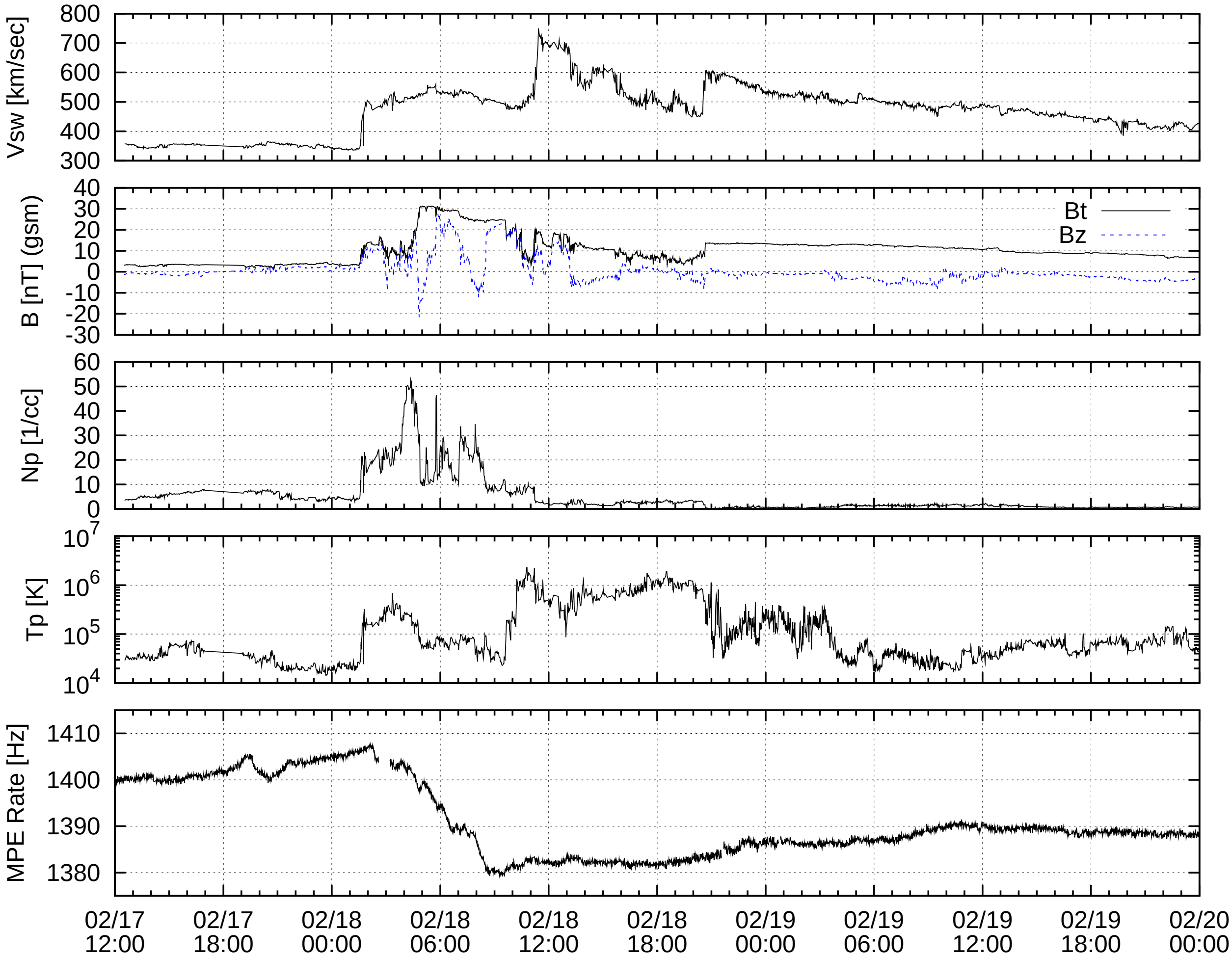

Figure 1: Observation of 18 February 2011 Forbush Decrease. From top to bottom are, solar wind speed, total component (Bt, solid line) and North-South component (Bz, dashed line) of interplanetary magnetic field, proton density, proton temperature, and average IceTop MPE scaler rate.

interplanetary magnetic field (IMF) in GSM coordinates, proton density and temperature of solar wind . The data plotted are primarily one-minute averaged high resolution OMNI data [3] from the *WIND* spacecraft. When *WIND* data are not available (18 February 20:40 UT to 19 February 9:50 UT) real-time *ACE* data [4], shifted by 50 minutes to correct for the time difference between satellite and Earth, are substituted. The time of the Storm Sudden Commencement (SSC) associated with the ICME-driven shock is at 18 February 01:30 UT. After the shock, the solar wind speed exceeds 700 km/s and IMF magnitude reaches 30 nT. Signatures of a magnetic cloud (strong magnetic field with smooth rotation, low proton temperature) are seen around the period 18 February 05:00 UT - 10:00 UT.

The lowest panel shows the pressure corrected average counting rate of all 146 MPE discriminators. The data in the figure is also averaged over one-minute, therefore the total count rate from 146 MPE discriminators for each data point displayed is ∼12 mega count/min. One can see not only the rapid decrease and gradual recovery of the Forbush decrease but a wealth of fine structure within the decrease. The onset of the Forbush decrease is 18 February 2:19 UT, which is ∼50 min later than the shock passage. Such a time lag between the SSC and onset of decrease is possibly caused by anisotropy of primary cosmic rays [5]. Just before 18 February 5:00 UT, there is a second decrease at the same time as the start of the magnetic cloud signature. This observation is consistent with the model of a classical two-step Forbush decrease [6]. The first step is caused by the turbulent sheath region behind the shock and the second step is caused by the entry into the enhanced and closed magnetic field of magnetic cloud (ejecta). The rate reaches minimum when Earth is located at the center of the magnetic cloud.

2.1 Rigidity Dependence of Forbush Decrease

We can track the evolution of the cosmic ray energy spectrum during the decrease by examining the time behavior as a function of discriminator threshold. Figure 2 shows the

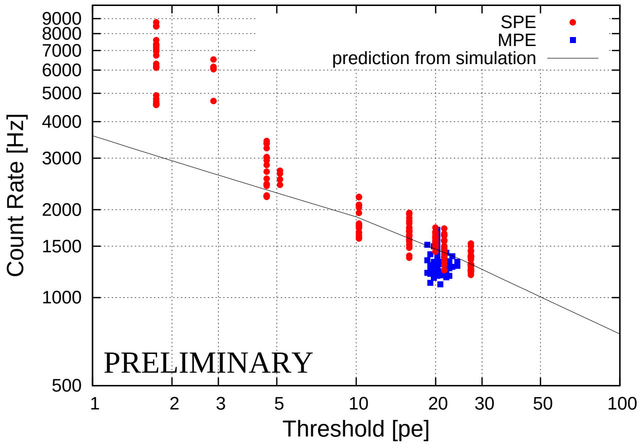

Figure 2: Count rate as a function of discriminator setting for the DOMs used in this study. Rates are averaged over the interval from 17 February 22:00 UT to 18 February 02:00, which defines the "base count rate" for the study. The line shows the expected values based on a simulation.

total counting rate as a function of threshold for the time interval prior to the event that we have chosen to determine the base count rate.

The energy dependence of the Forbush decrease is shown in Figure 3. The size of the decrease for each DOM is calculated as a percentage deviation from the base count rate. Four time periods in the main phase of Forbush decrease are plotted in the left panel, while four other time periods during the recovery phase are plotted in the right panel. The time periods corresponding to each measurement is shown in the figure. In the main phase, the first period is at the first step of the Forbush decrease, while the remaining three are in the second step until the maximum decrease. In the recovery phase, the day by day transition is shown. We confirm that the DOMs with higher count rate (lower threshold setting) have a larger decrease, as expected. This rigidity dependence is more remarkable in the recovery phase.

2.2 Estimation of primary spectrum variation by the Force-field model

To quantify the spectral changes during the event we use the force-field model [7, 8]. Although the force-field model basically describes the long term galactic cosmic ray modulation by the solar activity in the heliosphere, it provides a simple way to characterize the evolution during this transient.

We define the interstellar spectrum J^{IS} [1/(m^2 sr s MeV)] as a function of the particle rigidity P [GV] [9].

$$J^{IS}(P) = \frac{19 \cdot (P/P_0)^{-2.78}}{1 + (P_0/P)^2} \tag{1}$$

where P_0 = 1 GV. Then the spectrum near Earth is estimated as

$$J(P,\phi) = \left(\frac{P}{P+\phi}\right)^2 \frac{19 \cdot ((P+\phi)/P_0)^{-2.78}}{1 + (P_0/(P+\phi))^2} \tag{2}$$

where ϕ [MV] is the so-called modulation parameter.

The IceTop count rate at different PE thresholds is calculated by the convolution of the yield function $S_{pe}(P)$ [1] with the primary cosmic ray spectrum $J(P,\phi)$ defined above, as

$$N_{pe}(\phi) = \int S_{pe}(P) J(P,\phi) dP. \tag{3}$$

Then, by assuming ϕ_0 as the modulation level of the primary spectrum before the Forbush decrease the rate decrease during the event is described as a function of ϕ. In this paper the ϕ_0 is roughly set to the 300MV for the normal galactic cosmic ray spectrum at this solar minimum [10].

The derived decrease size at different time periods is shown with curves in Figure 3. Modulation parameters ϕ for each time period are given in the figure, which reach ϕ=406MV at the maximum decrease.

We notice that there are significant differences between the force-field model and the observed decrease for the high count rate DOMs, especially those set to thresholds less than 5 PE, shown as open symbols. Pre-event counting rates (Figure 2) for these thresholds are also significantly higher than the simulation model that is otherwise a good fit. The most likely explanation of this is background due to ambient radiation, but we have to this point not made an allowance for this in our models. Presence of a constant background would clearly reduce the size of the Forbush decrease as a percentage, which is how the data in Figure 3 are displayed. Similar effects were seen in our analysis of a solar flare event [11]. When more flare events, with varying spectra, are observed we will be able to derive self consistent corrections for this background.

Except for the high count rate DOMs, observed decreases in the main phase are well reproduced by the primary spectrum defined by the force-field model. This result suggests that it is indeed reasonable to apply the force-field approximation from the onset of the transient event [12] through the time of maximum decrease. However in the recovery phase the spectra become progressively less well fit by the force-field model. This quantifies the observation that higher energy galactic cosmic rays typically recover faster than lower energy ones, as observed by [5, 13].

3 Summary

IceTop observed the Forbush decrease event associated with the X2.2 solar flare in February, 2011. The high counting rate detector makes possible to observe the onset time of the Forbush decrease accurately. The rigidity dependence of the Forbush decrease is estimated by the detector response with the primary spectrum expected from

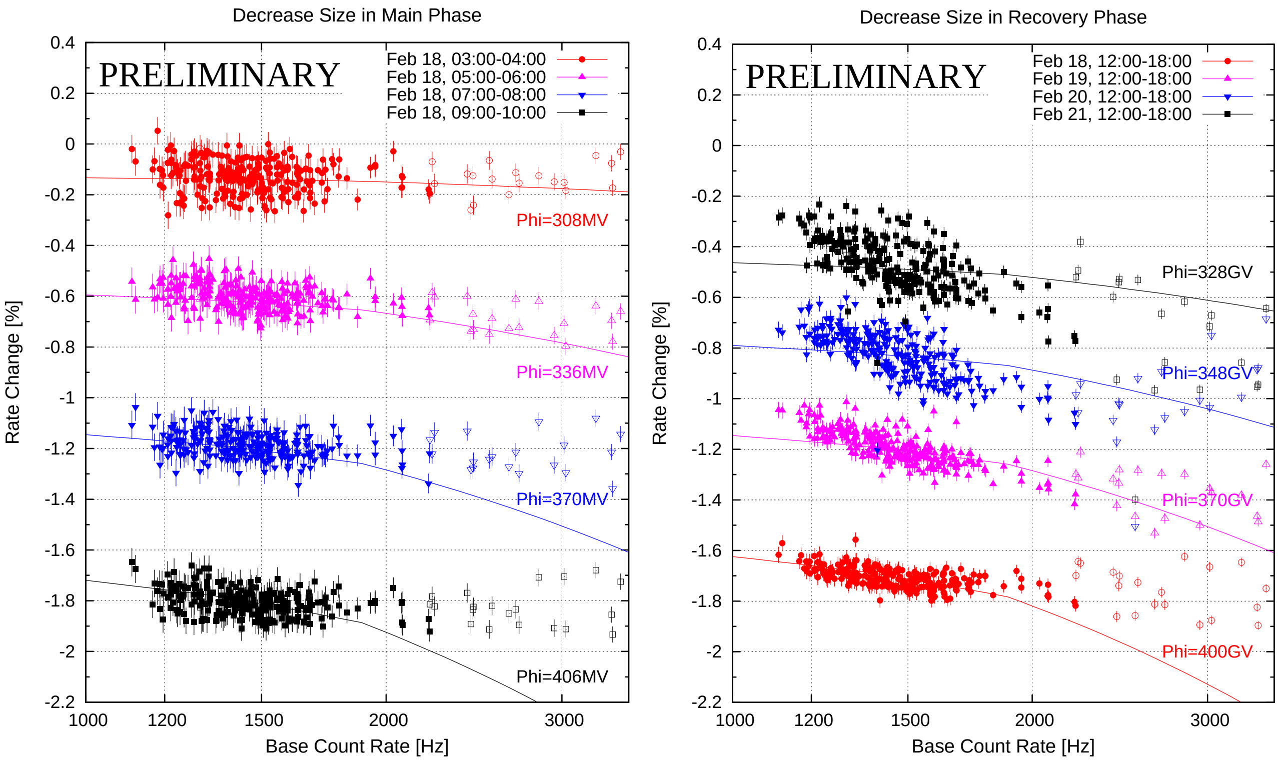

Figure 3: Decrease in counting rate for each DOM at different times during the main phase (left) and recovery phase (right) of the Forbush decrease. The decrease, expressed as a percentage of the base count rate, measured from 17 February 22:00 UT to 18 February 02:00 is plotted as a function of the base count rates. DOMs set to very low threshold ($\leq$5 PE) are shown as open symbols. Lines are expected decrease size calculated from force-field spectrum at the indicated modulation parameter ϕ.

the force-field approximation. The observed rigidity dependence of decrease size is well reproduced by the force-field primary spectrum during the main phase. By contrast, the strong rigidity dependence in the recovery phase of this event is not reproduced by it.

There are some problems remaining. The expected decrease sizes from the assumed primary spectrum overestimated the decrease in the high counting rate DOMs. Probably the counting rates of these DOMs includes background that is not accounted for in the calculation of the yield function. Our current yield function is not taking account of the effect of the different snow accumulation on the tanks either. Further work will be required to refine this. We should also note that the current analysis didn't correct for effects of the primary cosmic ray anisotropy.

Acknowledgements

The OMNI data were obtained from the GSFC/SPDF OMNIWeb interface. The ACE real time data were obtained from Space Weather Prediction Center.

References

[1] Clem, J. M., Niessen, P., Stoyanov, S. (2008). Proceedings of the 30th ICRC, Mérida, **1**, 237-240.
[2] Forbush, S. E. (1938), Phys. Rev., **54**, 975-988.
[3] http://omniweb.gsfc.nasa.gov
[4] http://www.swpc.noaa.gov/ace
[5] Lockwood, J. A. (1971), Space Sci. Revs. **12**, 658-715.
[6] Cane, H. V. (2000), Space Science Reviews, **93**(1/2), 55-77.
[7] Gleeson L. J. and I. H. Urch (1973), Space Sci., **25**, 387-404.
[8] Caballero-Lopez, R. A., and H. Moraal (2004), J. Geophys. Res., **109**, A01101.
[9] Burger, R. A., T. P. J. Krüger, M. Hitge and N. E. Engelbrecht (2008), Astrophys. J., **674**, 511.
[10] Usoskin, I. G., G. A. Bazilevskaya, and G. A. Kovaltsov (2011), J. Geophys. Res., **116**, A02104.
[11] Abbasi, R. et al., IceCube collaboration (2008), Astrophys. J. Lett., **689**, 65-68
[12] Ahluwalia, H. S., and M. M. Fikani (2007), J. Geophys. Res., **112**, A08105.
[13] Usoskin, I. G. et al. (2008), J. Geophys. Res., **113**, A07102.